Intelligence 87 (2021) 101545

Contents lists available at ScienceDirect

Intelligence

journal homepage: www.elsevier.com/locate/intell

Interindividual differences in matrix reasoning are linked to functional connectivity between brain regions nominated by Parieto-Frontal Integration Theory

Christoph Fraenz [a,*], Caroline Schlüter [b], Patrick Friedrich [c], Rex E. Jung [d], Onur Güntürkün [b], Erhan Genç [a]

[a] Department of Psychology and Neurosciences, Leibniz Research Centre for Working Environment and Human Factors (IfADo), 44139 Dortmund, Germany
[b] Department of Biopsychology, Ruhr University Bochum, 44801 Bochum, Germany
[c] Institut für Neurowissenschaften und Medizin, Forschungszentrum Jülich, 52425 Jülich, Germany
[d] Department of Neurosurgery, University of New Mexico, Albuquerque, NM 87131, USA

ARTICLE INFO

Keywords:
Resting-state fMRI
Functional connectivity
Matrix reasoning
Parieto-Frontal Integration Theory

ABSTRACT

The Parieto-Frontal Integration Theory (P-FIT) predicts that human intelligence is closely linked to structural and functional properties of several brain regions mainly located in the parietal and frontal cortices. It also proposes that solving abstract reasoning tasks involves multiple processing stages and thus requires the harmonic interplay of these brain regions. However, empirical studies directly investigating the relationship between intellectual performance and the strength of individual functional connections related to the P-FIT network are scarce. Here we demonstrate, in two independent samples comprising a total of 1489 healthy individuals, that fMRI resting-state connectivity, especially between P-FIT regions, is associated with interindividual differences in matrix reasoning performance. Interestingly, respective associations were only present in the overall samples and the female subsamples but not in the male subsamples, indicating a sex-specific effect. We found five statistically significant connections which replicated across both samples. These were constituted by BAs 8, 10, 22, 39, 46, and 47 in the left as well as BAs 44 and 45 in the right hemisphere. Given that many of these brain regions are predominantly involved in language processing, we hypothesized that our results reflect the importance of inner speech for solving matrix reasoning tasks. Complementary to previous research investigating the association between intelligence and functional brain connectivity by means of comprehensive network metrics, our study is the first to identify specific connections from the P-FIT network whose functional connectivity strength at rest can be considered an indicator of intellectual capability.

1. Introduction

Based on reliable scientific evidence accumulated over the course of more than a century, it is beyond dispute that individuals differ with regard to their intellectual abilities (Deary, 2012; Deary, Penke, & Johnson, 2010; Spearman, 1904). Since the dawn of intelligence research, it has been of considerable interest to establish a link between intellectual ability and the various properties of its underlying neural substrates within the human brain. Technical developments during the second half of the 20th century, such as magnetic resonance imaging and positron emission tomography, enabled researchers to assess a wide variety of structural and functional brain properties in vivo and investigate their relationship with intellectual abilities. According to evidence from this line of research, intelligence has been associated with numerous neural characteristics including brain volume (McDaniel, 2005; Pietschnig, Penke, Wicherts, Zeiler, & Voracek, 2015), cortical thickness (Karama et al., 2011; Narr et al., 2007), white matter integrity (Penke et al., 2012; Ritchie et al., 2015), structural connectivity (Li et al., 2009), task-based (Avery et al., 2020; Frith et al., 2021; Haier et al., 1988; Neubauer & Fink, 2009) and resting-state brain activity (Avery et al., 2020; Ezaki, Fonseca Dos Reis, Watanabe, Sakaki, & Masuda, 2020), as well as cortical microstructure (Genc et al., 2018). In

* Corresponding author at: Nachwuchsgruppe "Neuroimaging und interindividuelle Unterschiede", Leibniz-Institut für Arbeitsforschung an der TU Dortmund, Ardeystraße 67, 44139 Dortmund, Germany.
E-mail address: fraenz@ifado.de (C. Fraenz).

https://doi.org/10.1016/j.intell.2021.101545
Received 16 June 2019; Received in revised form 6 May 2021; Accepted 7 May 2021

line with the ever-growing arsenal of in vivo imaging techniques, the focus of neuroscientific approaches to intelligence research has shifted from the overall brain to single brain regions. However, converging evidence from a large body of literature indicates that intelligence is not tied to one particular brain region but related to the anatomical properties and functional activation patterns of multiple regions spread throughout the brain.

In this regard, Jung and Haier (2007) conducted a review of 37 studies featuring data obtained by various neuroimaging techniques. Their efforts led to the proposal of the Parieto-Frontal Integration Theory of intelligence (P-FIT). From the combined evidence, Jung and Haier identified a set of 14 Brodmann areas (BAs), in which different neural properties had been consistently linked to intelligence. These were mainly located in the dorsolateral prefrontal cortex, in the parietal lobule, in the anterior cingulate cortex and regions within the temporal and occipital lobes. The authors assumed that all P-FIT areas, even though they were identified independently of each other, had to be connected through a widespread network. Jung and Haier emphasized the fact that solving an abstract reasoning tasks involves multiple processing stages and thus requires the harmonic interplay of multiple brain regions. In more detail, the P-FIT model argues that intelligent thinking originates from the successful recognition and elaboration of information from sensory cortices. Consequentially, extrastriate cortex (BAs 18, 19) and temporal regions (BAs 21, 37) are hypothesized to be of prime importance for these first steps. Subsequently, structural symbolism and abstraction are believed to emerge from the supramarginal (BA 40), the superior parietal (BA 7), and the angular gyrus (BA 39). Following this, potential solutions to a given problem are thought be generated in frontal regions (BAs 6, 9, 10, 45, 46, 47) and fed forward to the anterior cingulate cortex (BA 32), which engages in a final response selection. This particular set of BAs was partially replicated and extended in a recent meta-analysis by Basten, Hilger, and Fiebach (2015). They identified six supplementary regions (BAs 8, 20, 24, 31, 42, 44) that were added to the original P-FIT network.

Given our present knowledge about the individual functions of P-FIT regions, it may seem plausible that they are organized in the network structure proposed by Jung and Haier (2007). However, this assumption has only been validated indirectly by previous research. The majority of these studies aimed to investigate the association between intelligence and functional brain network connectivity by means of fMRI resting-state data. This approach emanates from the idea that spontaneous fluctuations in the blood oxygenation level dependent (BOLD) signal contain information about the quality of evoked brain activity, e.g. mental effort exerted during reasoning (Fox & Raichle, 2007; Tavor et al., 2016). For example, Song et al. (2008) employed resting-state data to relate the functional connectivity strength between bilateral dorsolateral prefrontal cortices and various other brain regions to general intelligence. The authors observed multiple statistically significant connections, which were exclusively constituted by BAs from the extended P-FIT model (BAs 9, 10, 40, 46). In another study, van den Heuvel, Stam, Kahn, and Hulshoff Pol (2009) followed a graph theoretical approach in order to investigate the association between functional brain network properties and intellectual performance. Results showed a negative correlation between intelligence test scores and the characteristic path length of the resting-state brain network, indicating that intelligence is a function of how efficiently information is integrated between multiple brain regions. Again, these findings were mainly tied to P-FIT areas (BAs 7, 9, 10, 31 39, 40, 44, 45), albeit with an exploratory statistical threshold. In contrast, Hilger, Ekman, Fiebach, and Basten (2017a) were not able to replicate these findings. With regard to the entire resting-state brain network, the authors did not observe a significant association between general intelligence and global efficiency, a graph measure inversely related to characteristic path length. In view of individual network nodes, three brain areas showed significant effects but only one of them, namely the dorsal anterior cingulate cortex (BA 32), could clearly be assigned to the P-FIT model. Yet another study by Hilger, Ekman, Fiebach, and Basten (2017b) employed graph analysis to investigate whether and how the brain's modular organization is associated with general intelligence. Again, no significant effects were found for global modularity features of the resting-state brain network. However, the authors identified several network nodes, in which between-module and/or within-module connectivity could be related to general intelligence. The majority of these nodes comprised areas from the extended P-FIT model (BAs 6, 7, 8, 9, 10, 18, 39, 40, 44, 47). One of the largest studies investigating the association between general intelligence and global functional network efficiency by means of graph analysis was conducted by Kruschwitz, Waller, Daedelow, Walter, and Veer (2018). The authors employed functional imaging data provided by the Human Connectome Project (Van Essen et al., 2013) and used various network definition schemes to relate measures of general, crystallized, and fluid intelligence to different global graph metrics, namely global efficiency, characteristic path length, and global clustering coefficient. Contrary to van den Heuvel et al. (2009), but in line with Hilger et al. (2017a) and Hilger et al. (2017b), the global approach used by Kruschwitz et al. (2018) did not yield any robust associations and only very weak non-significant effects. Using independent component analysis, Vakhtin, Ryman, Flores, and Jung (2014) managed to identify a total of 29 functional networks in two independent sets of fMRI data. The first set was obtained while participants were at rest and the second while participants were solving a matrix reasoning task. Out of all functional networks, 26 were present in both datasets, supporting the idea that spontaneous fluctuations in the BOLD signal are informative of task-based brain activity. Notably, 10 functional networks, which were broadly consistent with the P-FIT model, were correlated with the matrix reasoning test scores. Santarnecchi et al. (2017) utilized fMRI resting-state data from a large sample in order to investigate the properties of a functional network (BAs 6, 7, 9, 10, 18, 32, 40, 46, 47) underlying fluid intelligence (Santarnecchi, Emmendorfer, & Pascual-Leone, 2017). Results showed that left inferior frontal (BAs 6, 9) and left inferior parietal regions (BA 40) exerted high connectivity with the rest of the network, indicating a pivotal role of these P-FIT areas in fluid intelligence. Furthermore, the authors generated a seed-based connectivity map between the fluid intelligence network and the rest of the brain. The respective map exhibited a high degree of similarity with three other major parieto-frontal resting-state networks. Dubois, Galdi, Paul, and Adolphs (2018) investigated the relationship between general intelligence and functional connectivity by analyzing fMRI resting-state data provided by the Human Connectome Project (Van Essen et al., 2013). The authors demonstrated that about 20% of variance in general intelligence can be explained when considering the entire connectivity matrix of each participant. When restricting the analysis to the most predictive edges, particular resting-state networks, namely the fronto-parietal network, the default mode network, the control network, and the visual network, turned out to carry more information than others. Respective results were found to be in general agreement with the P-FIT model. Another study employing the Human Connectome Project's dataset was conducted by Finn et al. (2015). More specifically, the authors used fMRI resting-state data recorded on two separate days to demonstrate that it is possible to match the two connectivity matrices of a participant with more than 90% accuracy. When restricting this identification procedure to edges from parieto-frontal regions, accuracy increased to almost 100%. In addition to that, the authors used the resting-state data to create linear regression models for the purpose of predicting matrix reasoning performance. Predicted scores were highly correlated with observed scores. Again, this association was mainly driven by edges constituting parieto-frontal networks similar to the P-FIT model.

Based on these findings, one can conclude that the general idea of P-FIT areas constituting a functionally connected network rests on a solid foundation of empirical evidence. However, none of the aforementioned studies was exclusively targeted at investigating the association between intelligence and the properties of individual functional connections from

the P-FIT network. Consequentially, previous research is limited to some extent. For example, Song et al. (2008) refrained from examining a network spanning the whole brain but focused on functional connectivity emanating from a priori defined seed regions in the dorsolateral prefrontal cortices. Other studies used graph theoretical measures in order to quantify functional connectivity (Hilger et al., 2017a, 2017b; van den Heuvel et al., 2009). Graph theory offers various metrics which capture the overall quality of a brain network or highlight the importance of particular nodes that contribute to the network's connectivity. However, these metrics are computed by aggregating information from all individual connections constituting the brain network. Hence, results obtained by this method only provide limited insight regarding the the properties of individual connections. In many cases (Dubois et al., 2018; Finn et al., 2015; Santarnecchi, Emmendorfer, & Pascual-Leone, 2017; Santarnecchi, Emmendorfer, Tadayon, et al., 2017), other networks than the P-FIT network were used as the prime object of investigation and P-FIT was merely used as the theoretical framework to interpret results, e.g. functional connectivity patterns observed in parieto-frontal regions. Due to these reasons, it remains unclear whether intelligence is related to the functional connectivity strength of individual connections nominated by the P-FIT model.

With the study at hand, we aimed to close this gap of knowledge by testing following three hypotheses. First, the P-FIT model promotes the idea that brain regions related to intelligence are organized in a functional network through which information is exchanged. Based on the research presented above, it is conceivable that efficient information exchange relies on a brain infrastructure that fosters high functional coherence between brain regions even in their resting state. Following this assumption, we hypothesized that higher BOLD signal correlations observed at rest would be associated with better performance on a matrix reasoning test. Hence, we analyzed the resting-state properties of functional connections included in the P-FIT network, but also of those spanning the rest of the brain. We expected significant associations between functional connectivity strength and matrix reasoning performance to be predominantly exhibited by connections from the P-FIT network and to a lesser degree by connections unrelated to the P-FIT model.

Second, Jung and Haier (2007) suggested a serial flow of information through the P-FIT network when engaging in abstract reasoning. With regard to this concept, we hypothesized that the majority of connections, expressing significant associations between functional connectivity strength and matrix reasoning performance, would conform to this pattern. In more detail, we expected the trajectory of respective connections to match one of the steps proposed by the serial flow information model, i.e. from visual/temporal areas to parietal areas, from parietal areas to frontal areas, and from frontal areas to the cingulate cortex. Accordingly, we assumed that the strength of functional connections omitting some of the aforementioned steps, e.g. by directly linking visual and frontal areas, would not be significantly associated with matrix reasoning performance or exhibit weaker correlations. In previous research, functional resting-state correlations have already been used to identify serial flow of information in the visual system (Genc, Schoelvinck, Bergmann, Singer, & Kohler, 2016).

Third, Jung and Haier (2007) did not make any assumptions regarding the absence of particular functional connections within the P-FIT network. Intellectual performance can benefit from an exchange of relevant information between brain areas since it has a positive impact on signal-to-noise ratio. However, it has also been suggested that mental capacity might be fostered by neural architectures built to filter out or shield themselves against irrelevant information (Genc et al., 2018). Avoiding unnecessary crosstalk between specific brain areas might lead to substantial decreases in a system's level of noise. Respective processes should be represented by negative correlations between intelligence and the functional connectivity strength between two brain areas. Given that such inverse relationships have been reported in previous research (Hilger et al., 2017b; Song et al., 2008), we assumed that they should also be found for the P-FIT network. Hence, we hypothesized to observe both positive and negative associations in our analyses.

In order to test these hypotheses, we employed data from two large samples, one recruited by ourselves and one provided by the Human Connectome Project (Van Essen et al., 2013). To the best of our knowledge, we present the first study to directly examine all possible functional connections from the entire Brodmann atlas in order to investigate whether matrix reasoning performance is significantly associated with the functional connectivity strength of individual connections from the P-FIT network.

2. Materials and methods

2.1. Participants in the S498 sample

The first sample, hereinafter referred to as sample S498, was recruited at Ruhr-University Bochum in Germany. Subjects were either paid for their participation or received course credit. All of them were naive to the purpose of the study and had no former experience with the administered matrix reasoning test. All participants had normal or corrected-to-normal vision and hearing, matched the standard inclusion criteria for fMRI examinations, and declared to have no history of psychiatric or neurological disorders. Each participant completed both the matrix-reasoning test and neuroimaging session described below. In total, we recruited 557 participants. Within this group, 503 participants were right-handed and 54 (9.69%) were left-handed as measured by the Edinburgh Handedness Inventory (Oldfield, 1971). This ratio is representative of the human population (Raymond & Pontier, 2004). Given that handedness has been shown to affect brain organization (Amunts et al., 1996; Amunts, Jäncke, Mohlberg, Steinmetz, & Zilles, 2000), we decided to exclude all left-handed subjects from our analysis. Within the remaining group of 503 participants, matrix reasoning test scores were checked for outliers as defined by Tukey's fences (Tukey, 1977), i.e. observations 1.5 interquartile ranges below the first or above the third quartile, and respective cases were removed from the dataset accordingly. As a consequence, five participants had to be excluded. Thus, all of the reported analyses were performed on the remaining data from 498 participants (245 males) between 18 and 72 years of age ($M = 27.41$, $SD = 9.37$). We utilized G*Power (Faul, Erdfelder, Buchner, & Lang, 2009) in order to compute the achieved power of our final sample post hoc. The analysis was based on a bivariate normal model for correlations and an effect size of $r = 0.15$ since this was about the average magnitude of correlation coefficients in the S498 sample. We set α to 0.05 and determined testing to be two-tailed. Based on these parameters, the analysis yielded a statistical power of 0.92, which indicates sufficient sample size. The study was approved by the local ethics committee of the Faculty of Psychology at Ruhr-University Bochum. All participants gave their written informed consent and were treated in accordance with the declaration of Helsinki.

2.2. Participants in the S991 sample

In order to validate the results obtained from the S498 sample, we downloaded data provided by the Human Connectome Project, namely the S1200 release (Van Essen et al., 2013). We obtained 1088 participants with data suitable for our analyses from the "Structural Preprocessed" and "Resting State fMRI 1 Preprocessed" packages. As with sample S498, we removed all left-handed participants ($n = 97$, 8.9%) from our analysis. Matrix reasoning test scores of the remaining participants were checked for outliers but none were found. Thus, no further participants were excluded and all of the reported analyses were performed on data from 991 subjects (447 males) between 22 and 36 years of age ($M = 28.78$, $SD = 3.70$). Again, we utilized G*Power in order to compute the statistical power achieved by this sample post hoc. Based on the sample size of 991 participants and the same parameters used for sample S498, the analysis resulted in an achieved power that

was above 0.99.

2.3. Acquisition of behavioral data in the S498 sample

The acquisition of behavioral data was conducted in a group setting of up to six participants, seated at individual tables, in a quiet and well-lit room. Matrix reasoning performance was measured with a German matrix-reasoning test called Bochumer Matrizentest (BOMAT) (Hossiep, Hasella, & Turck, 2001), which is widely used in neuroscientific research (Genc et al., 2018; Klingberg, 2010; Oelhafen et al., 2013). The test examines non-verbal mental abilities that contribute to intelligence and is similar to Raven's Advanced Progressive Matrices (Raven, Raven, & Court, 2003). We conducted the "advanced short version" of the BOMAT, which has the advantage of high discriminatory power in samples with generally high intellectual abilities, thus avoiding possible ceiling effects (Genc et al., 2018). The BOMAT inventory comprises two parallel test forms (A and B) with 29 matrix-reasoning items each. Participants had to complete only one of the two test forms, which were randomly assigned. Split-half reliability of the BOMAT is 0.89, Cronbach's α is 0.92 and parallel-forms reliability between A and B is 0.86 (Hossiep et al., 2001). Additionally, convergent and predictive validity are given for both BOMAT test forms since they are strongly correlated with other intelligence inventories ($r = 0.59$), tests of perceptual speed ($r = 0.51$), and German high school GPA ($r = -0.35$) (Hossiep et al., 2001). The recent norming sample consists of about 2100 individuals with an age range between 18 and 60 years and equal sex representation.

2.4. Acquisition of behavioral data in the S991 sample

In sample S991, matrix reasoning performance was measured with the Penn Matrix Analysis Test (PMAT24) (Moore, Reise, Gur, Hakonarson, & Gur, 2015). This instrument is included in the Computerized Neuropsychological Test Battery provided by the University of Pennsylvania (PennCNP). The PMAT24 is an abbreviated version of the Raven's Progressive Matrices and includes 24 items of increasing difficulty. Each matrix pattern is made up of 2×2, 3×3, or 1×5 arrangements of squares with one of the squares missing. The participant must pick one of five response choices that best fits the missing square on the pattern. There is no time limit to the completion of the test, although the task discontinues if the participant makes five incorrect responses in a row. The PMAT24 has two test forms of which the Human Connectome Project only used one (form A) in order to assess matrix reasoning performance.

2.5. Acquisition of imaging data in the S498 sample

All imaging data were acquired at the Bergmannsheil hospital in Bochum (Germany) using a Philips 3T Achieva scanner with a 32-channel head coil. For the purpose of segmenting brain scans into gray and white matter segments as well as for the identification of anatomical landmarks, a T1-weighted high-resolution anatomical image was acquired (MP-RAGE, TR = 8.2 ms, TE = 3.7 ms, flip angle = 8°, 220 slices, matrix size = 240 × 240, voxel size = 1 × 1 × 1 mm). The acquisition time of the anatomical image was 6 min. For the analysis of functional connectivity, fMRI resting-state data were acquired using echo planar imaging (TR = 2000 ms, TE = 30 ms, flip angle = 90°, 37 slices, matrix size = 80 × 80, resolution = 3 × 3 × 3 mm). Participants were instructed to lay still with their eyes closed and to think of nothing in particular. The acquisition time of the resting-state images was 7 min.

2.6. Acquisition of imaging data in the S991 sample

All imaging data included in the S991 sample were acquired on a customized Siemens 3T Connectome Skyra scanner housed at Washington University in St. Louis using a standard 32-channel Siemens receive head coil. The Human Connectome Project's imaging hardware and protocols are documented elaborately in several publications (Smith et al., 2013; Van Essen et al., 2012; Van Essen et al., 2013) as well as the reference manual for the S1200 release. Anatomical and functional imaging were carried out in the same session with a mock scanner practice preceding the anatomical imaging. A T1-weighted high-resolution anatomical image was acquired by means of an MP-RAGE sequence and the following parameters: TR = 2400 ms, TE = 2.14 ms, flip angle = 8°, matrix size = 224 × 224, voxel size = 0.7 × 0.7 × 0.7 mm. The acquisition time of anatomical imaging was 7 min and 40 s. Functional resting-state imaging was carried out using multiband accelerated echo planar imaging with a multiband factor of eight (TR = 700 ms, TE = 33 ms, flip angle = 52°, 72 slices, matrix size = 104 × 90, resolution = 2 × 2 × 2 mm). Cardiac and respiratory signals were recorded at a sampling rate of 400 Hz using a pulse oximeter and respiratory bellows that were fitted to participants prior to the fMRI scans. In order to prevent the subjects from falling asleep during scanning, they were asked to keep their eyes open and fixate on a white cross while thinking of nothing in particular. For each participant, the Human Connectome Project provides a total of four 15-min resting-state scans, of which the first two scans were recorded during the participant's first visit to the scanning site, while the other two were recorded during the participant's second visit on a separate day. In order to ensure maximum comparability between the S498 and the S991 samples, we refrained from analyzing imaging data collected on two separate days and merely included the first two scans provided by the Human Connectome Project. These two scans were acquired with opposite phase-encoding directions. Total acquisition time of resting-state fMRI was 30 min.

2.7. Analysis of imaging data in the S498 sample

In order to reconstruct the cortical surfaces of the T1-weighted images we used published surface-based methods in FreeSurfer (http://surfer.nmr.mgh.harvard.edu, version 5.3.0). The details of this procedure have been described elsewhere (Dale, Fischl, & Sereno, 1999; Fischl, Sereno, & Dale, 1999). The automated reconstruction steps included skull stripping, gray and white matter segmentation as well as reconstruction and inflation of the cortical surface. After preprocessing, each individual segmentation was quality-controlled slice by slice and any inaccuracies were corrected by manual editing if necessary. In addition to gray and white matter masks, FreeSurfer's automated brain segmentation also yielded various ventricle masks and a cortical parcellation based on the PALS-B12 atlas (Van Essen, 2005), which in turn is based on the cytoarchitectonic areas defined by Brodmann (1909). It has to be noted that there are more sophisticated parcellation schemes which comprise a substantially higher number of individual brain regions compared to Brodmann's delineation of the cortex (Genc et al., 2018; Glasser et al., 2016; Power et al., 2011; Shen, Tokoglu, Papademetris, & Constable, 2013). However, since the original P-FIT model was defined using BAs, we decided to utilize the same segmentation in order to ensure high comparability between our analyses and the model we wanted to investigate. The PALS-B12 atlas was provided in the form of annotation files comprising a total of 82 brain regions that had to be converted to volumetric masks. In a final step, the two segments delineating the overall cortex and white matter as well as the ventricle masks and all 82 masks representing single BAs were linearly transformed into the native space of the resting-state images (Fig. 1).

The transformed regions served as anatomical landmarks from which average BOLD signal timecourses were extracted. Resting-state data were preprocessed using MELODIC, which is part of the FSL toolbox. The first two EPI volumes were discarded from each resting-state scan to allow for signal equilibration. Motion and slice-timing correction as well as high-pass temporal frequency filtering (0.005 Hz) were applied. In order to avoid spurious correlations in neighboring voxels, spatial smoothing was not applied.

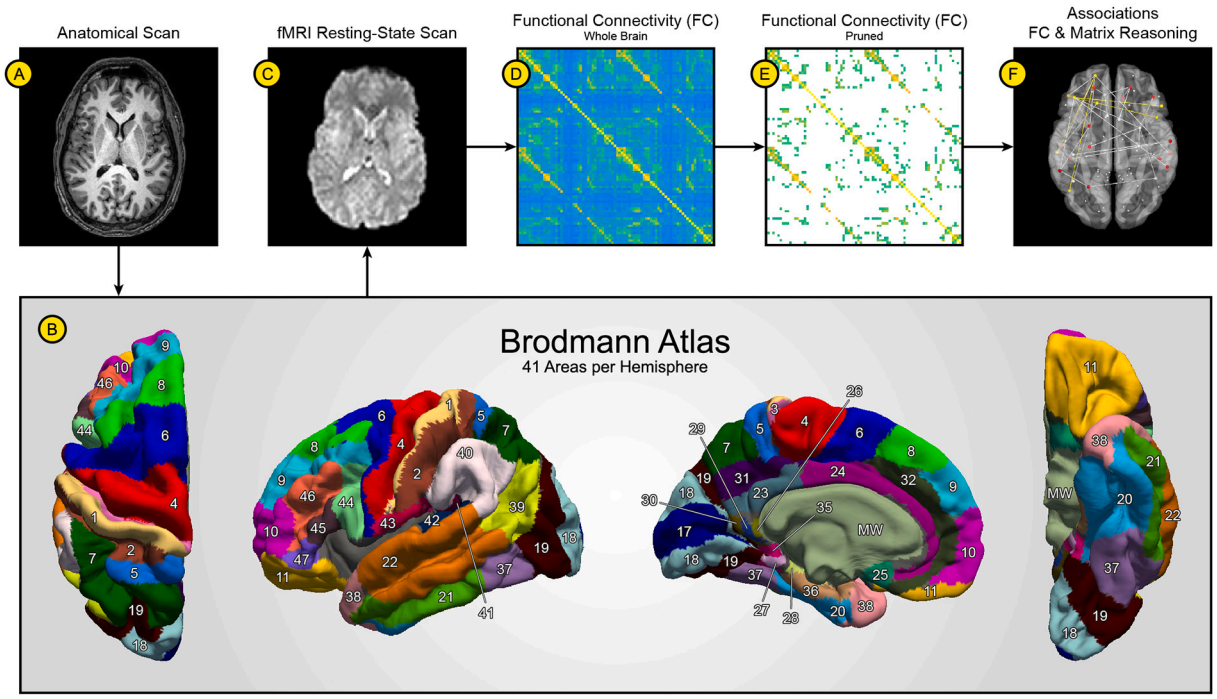

Fig. 1. Methodological sequence for the parcellation of brain scans, the computation of resting-state connectivity matrices, and the analysis of associations between functional connectivity and matrix reasoning performance. T1-weighted anatomical scans (A) were delineated into 41 areas per hemisphere based on the Brodmann atlas implemented in FreeSurfer (B). Respective brain masks were linearly transformed into the native space of resting-state images (C). For the purpose of creating functional connectivity matrices (D), partial correlations between the average BOLD signal timecourses of all Brodmann areas were computed. Head movement and average BOLD signal timecourses from white matter structures and ventricles were used as controlling variables. Pruned versions of these functional connectivity matrices (E) were obtained by removing all cells in which correlation coefficients failed to reach statistical significance ($p < .05$) in 90% of subjects across both samples. The remaining correlation coefficients were subjected to Fisher z-transformations and employed to compute partial correlations with matrix reasoning test scores (F). Head movement and age were used as controlling variables. Within the S498 and the S991 sample, analyses were carried out for the entirety of subjects and for both sexes separately.

2.8. Analysis of imaging data in the S991 sample

The preprocessing of anatomical and functional data from the S991 sample was carried out according to the Human Connectome Project's minimal preprocessing pipelines (Glasser et al., 2013). Importantly, this pipeline also aims to minimize the smoothing from interpolation and does not involve any overt volume smoothing. We applied the same steps as used for the S498 sample in order to generate volumetric masks, representing overall cortex, white matter, ventricles and BAs, from the T1-weighted anatomical images. Finally, all respective masks were linearly transformed into the native space of resting-state images and average BOLD signal timecourses were extracted. In order to combine our analyses across the two 15-min runs obtained for every participant, we followed an approach suggested by the Human Connectome Project (Smith et al., 2013) and simply concatenated each timeseries encoded in the right-left direction with its respective counterpart encoded in the left-right direction.

2.9. Statistical analysis

All statistical analyses were carried out using MATLAB version R2020b (The MathWorks Inc., Natick, MA). For the purpose of generating functional connectivity matrices and relating them to matrix reasoning test scores, we used linear parametric methods. Testing was always two-tailed with an α-level of 0.05, which we eventually corrected for multiple comparisons using the Benjamini-Hochberg method (Benjamini & Hochberg, 1995). For every participant we computed partial correlation coefficients between the average BOLD signal timecourses of all BAs while controlling for several nuisance variables. We regressed out the trajectories of all six motion parameters as well as the mean timecourses averaged across voxels representing white matter or cerebro-spinal fluid (Genc et al., 2016). This resulted in a symmetrical 82-by-82 matrix for each participant with partial correlation coefficients representing the functional connectivity of 3321 individual resting-state connections (one matrix triangle without self-connections on the diagonal). By applying Fisher z-transformation to all values (Fisher, 1921), we ensured that these partial correlation coefficients were normally distributed. In order to remove spurious functional connections from our analyses, we created a pruned version of each participant's connectivity matrix (Song et al., 2008). All network edges, i.e. cells containing normalized BOLD signal correlations, that did not reach statistical significance in 90% of subjects across both samples, were discarded. Only the remaining portion of each participant's connectivity matrix was considered for further analyses. In the S498 sample, we computed partial correlation coefficients between functional connectivity values and BOMAT test scores while controlling for the effects of age and in-scanner head motion in terms of mean framewise displacement. In the S991 sample, we proceeded in the same manner but used PMAT24 test scores. In both cases, the resulting test statistics were corrected for multiple comparisons using the Benjamini-Hochberg method. Finally, all functional connections which exhibited significant associations between their normalized BOLD signal correlations and the matrix reasoning test scores across both samples were subjected to multiple regression analysis. Here, normalized BOLD signal correlations of the selected connections served as independent variables and matrix reasoning test scores were used as the independent variable. Firstly, single regression models including all participants of a sample were computed for the S498 and S991 datasets, respectively. Secondly, regression models based on randomly picked subsamples with only 75% of subjects were computed in iterative fashion (10,000 analyses per group) and test

statistics were averaged across all iterations. We conducted aforementioned analyses for the entirety of each sample as well as separately for male and female participants.

2.10. Data and code availability

The data and MATLAB code that support the findings of this study are available from the corresponding author upon reasonable request or can be downloaded from an Open Science Framework repository [https://osf.io/xb4mc/]. The data used for sample S991 are part of the S1200 release provided by the Human Connectome Project and can be accessed via its ConnectomeDB platform [https://db.humanconnectome.org/].

3. Results

For sample S498, functional resting-state connectivity exhibited by 3321 individual connections is illustrated as a symmetrical 82-by-82 matrix in Supplementary Fig. 1. The respective matrix was obtained by averaging all individual connectivity matrices from sample S498. In a subsequent step, potentially spurious functional connections were removed from each participant's connectivity matrix by discarding all cells in which normalized BOLD signal correlations failed to reach statistical significance in 90% of subjects across both samples. Thereby, 2920 individual functional connections were excluded from further analysis and only 401 connections (12.07%) remained (counting only one triangle of the matrix without self-connections on the diagonal). Notably, none of the negative correlation coefficients survived this pruning procedure. For sample S498, the pruned version of the mean connectivity matrix is presented in Supplementary Fig. 2. In order to test whether functional connectivity at rest was associated with matrix reasoning performance, we correlated the remaining functional connectivity values with BOMAT test scores, while controlling for the effects of age and in-scanner head motion (Fig. 2).

While the resulting partial correlation coefficients were in the range of −0.07 to 0.19 and thus indicated both negative and positive associations, the majority of associations was positive (364 out of 401, 90.77%). After correcting for multiple comparisons, the partial correlation coefficients in 31 functional connections still reached statistical significance (7.73%, $r = 0.13–0.19$). Twenty out of these 31 connections were exclusively constituted of BAs from the P-FIT network (64.52%). Nine connections ran between a BA from the P-FIT network and a BA unrelated to P-FIT (29.03%). Out of all connections for which functional connectivity was significantly associated with BOMAT test scores, we

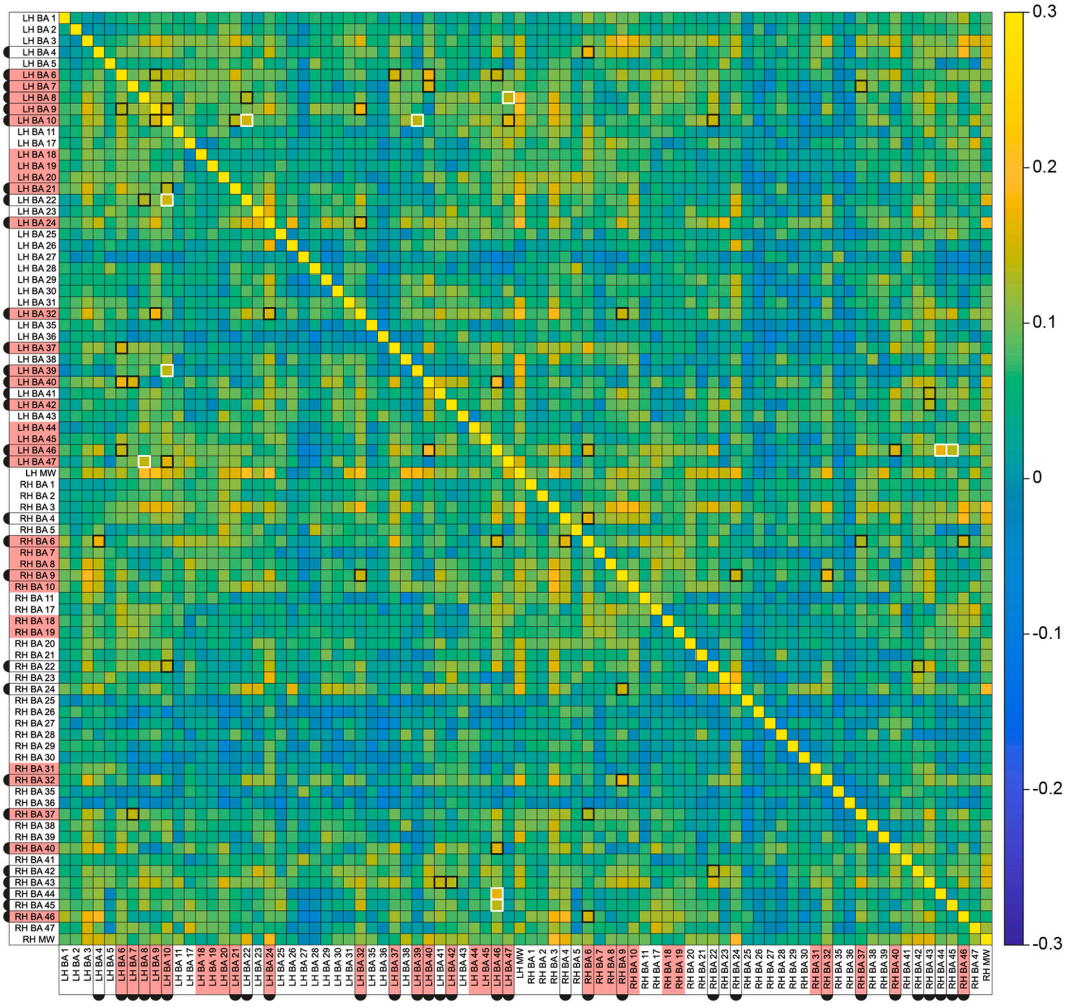

Fig. 2. Symmetrical 82-by-82 matrix visualizing the association between functional connectivity and matrix reasoning performance for 3321 individual connections in sample S498. All cells representing associations that reached statistical significance after correction for multiple comparisons are highlighted with black boxes. Significant associations replicating across both samples (S498 and S991) are highlighted with white boxes. Brodmann areas that belong to the extended P-FIT network are highlighted in red. Brodmann areas constituting functional connections significantly associated with matrix reasoning performance are framed in black and marked by black half circles. LH = left hemisphere, RH = right hemisphere, BA = Brodmann area, MW = medial wall. (For interpretation of the references to colour in this figure legend, the reader is referred to the web version of this article.)

only observed two that did not involve at least one BA from the P-FIT network (6.45%). Altogether, we identified 15 intrahemispheric connections in the left hemisphere (48.39%), six intrahemispheric connections in the right hemisphere (19.35%), and 10 interhemispheric connections (32.26%) (Fig. 3).

Data from the S991 sample were analyzed in accordance with the approach followed for the S498 sample. Again, functional connectivity between BAs is illustrated by symmetrical 82-by-82 matrices, one representing the entire network (Supplementary Fig. 3) and one representing its pruned version (Supplementary Fig. 4). For each of the 401 individual connections in sample S991 functional connectivity values were correlated with PMAT24 test scores, while controlling for the effects of age and in-scanner head motion (Fig. 4).

As with sample 498, the resulting partial correlation coefficients indicated both negative and positive associations, this time in the range of −0.05 to 0.15. Further, the number of connections expressing positive associations between functional connectivity and PMAT24 test scores (337 out of 401, 84.04%) was comparable to the S498 sample. Forty-three of these partial correlation coefficients, all of them positive, survived a correction for multiple comparisons and still reached statistical significance (10.72%, r = 0.09–0.15). As with sample S498, most statistically significant connections were exclusively constituted of BAs from the P-FIT network (17 out of 43, 39.53%). We found 15 statistically significant connections which ran between one BA from the P-FIT network and one unrelated BA (34.88%). Lastly, we observed 11 statistically significant connections between BAs completely unrelated to the P-FIT network (25.58%). The 43 statistically significant connections included 12 intrahemispheric connections in the left hemisphere (27.91%), 11 intrahemispheric connections in the right hemisphere (25.58%), and 20 interhemispheric connections (46.51%) (Fig. 5).

Five statistically significant connections were present in both samples. Among these were three intrahemispheric connections in the left hemisphere, namely one between BAs 8 and 47 (S498: $r = 0.14$, $p < .01$; S991: r = 0.09, $p < .01$), one between BAs 10 and 22 (S498: $r = 0.15$, $p < .001$; S991: r = 0.13, $p < .001$), and one between BAs 10 and 39 (S498: r = 0.14, $p < .01$; S991: $r = 0.12$, $p < .001$). Moreover, there were two interhemispheric connections, namely one between BA 46 in the left and BA 44 in the right hemisphere (S498: $r = 0.17$, $p < .001$; S991: $r = 0.10$, $p < .01$) as well as one between BA 46 in the left and BA 45 in the right hemisphere (S498: r = 0.14, $p < .01$; S991: r = 0.09, $p < .01$). The connections between BAs 8 and 47 as well as BAs 10 and 39 were exclusively constituted by areas nominated by the P-FIT model, whereas each of the remaining three connections included one related (BAs 10, 46) and one unrelated area (BAs 22, 44, 45). In addition to the five

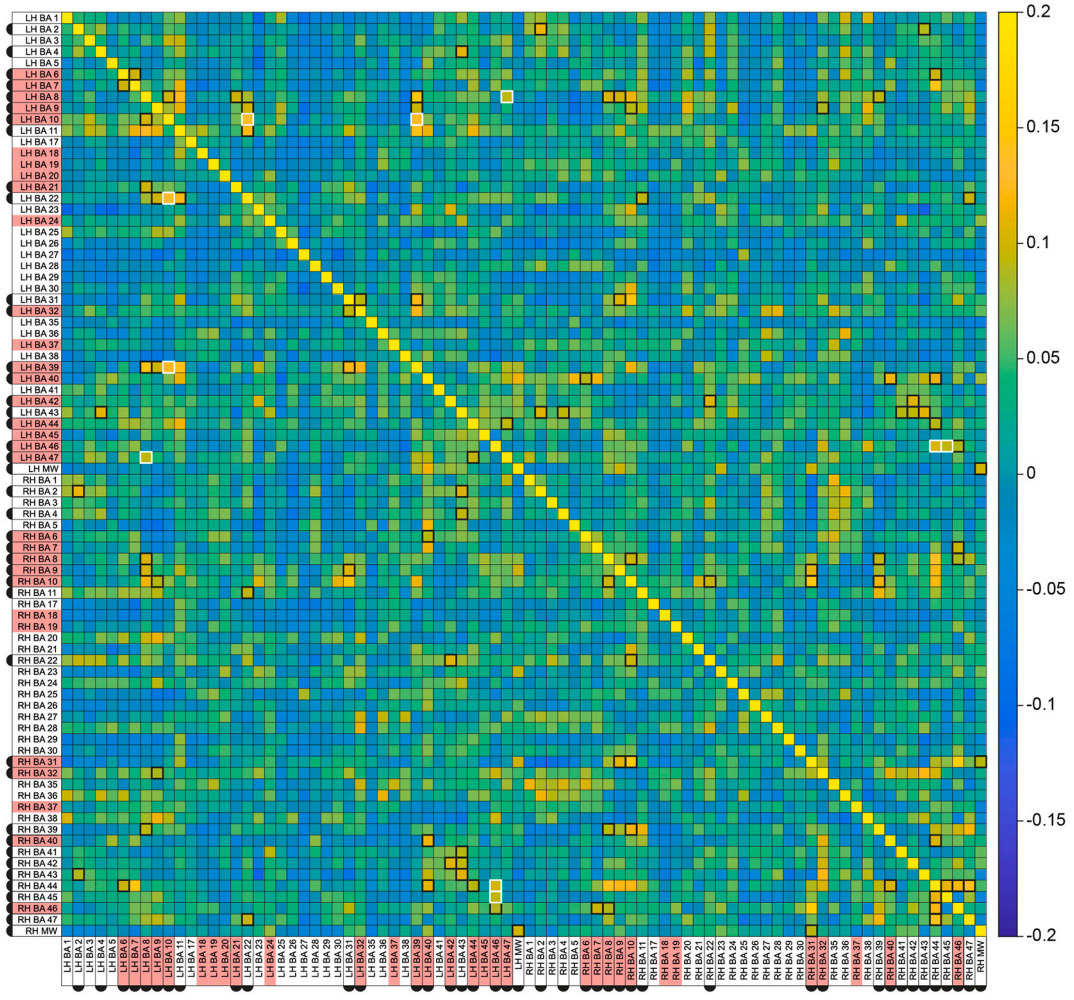

Fig. 3. Symmetrical 82-by-82 matrix visualizing the association between functional connectivity and matrix reasoning performance for 3321 individual connections in sample S991. All cells representing associations that reached statistical significance after correction for multiple comparisons are highlighted with black boxes. Significant associations replicating across both samples (S498 and S991) are highlighted with white boxes. Brodmann areas that belong to the extended P-FIT network are highlighted in red. Brodmann areas constituting functional connections significantly associated with matrix reasoning performance are framed in black and marked by black half circles. LH = left hemisphere, RH = right hemisphere, BA = Brodmann area, MW = medial wall. (For interpretation of the references to colour in this figure legend, the reader is referred to the web version of this article.)

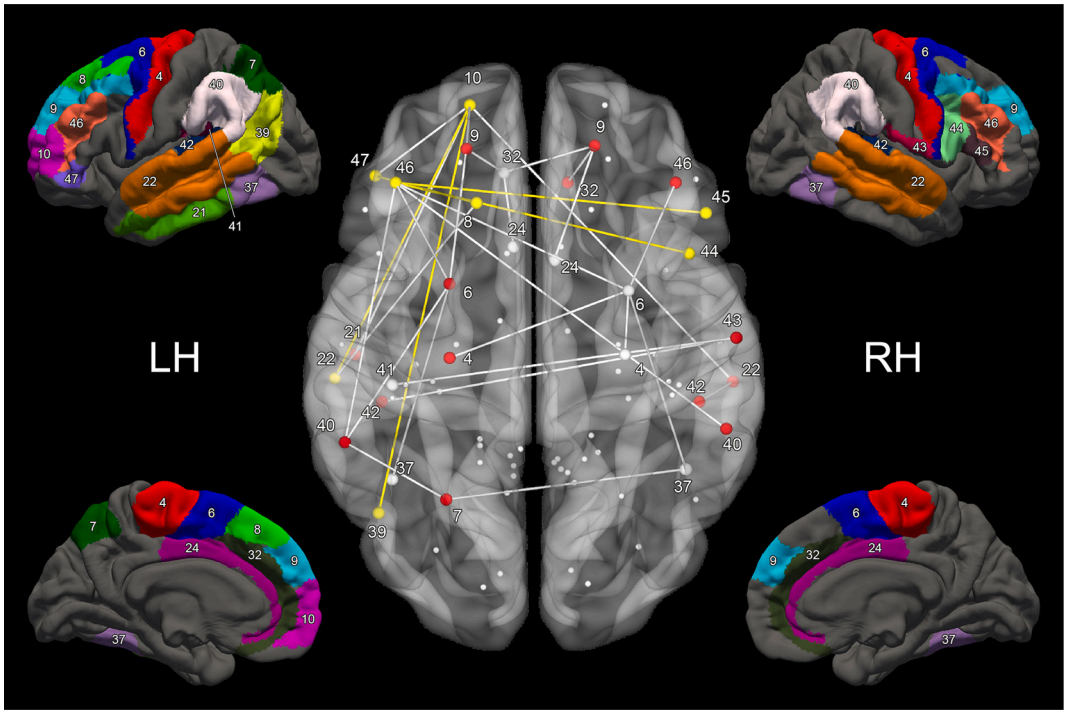

Fig. 4. Schematic depiction of functional connections showing statistically significant associations with matrix reasoning performance in sample S498. Brodmann areas included in the parcellation scheme used for this study are shown as white spheres within the semi-transparent MNI brain in the center. Functional connections exerting statistically significant correlations between their connectivity strength and matrix reasoning performance are shown as white lines. Spheres constituting statistically significant connections are slightly bigger than the rest and carry labels with the numbers of their corresponding Brodmann areas. Spheres and lines representing functional connections which replicated across both samples (S498 and S991) are depicted in yellow. Brodmann areas which were involved in statistically significant connections in both samples are represented by red spheres. All Brodmann areas constituting statistically significant connections are also shown as colored labels on four brain surfaces in the corners (lateral and medial views of the left and right hemispheres). (For interpretation of the references to colour in this figure legend, the reader is referred to the web version of this article.)

connections which replicated across both samples, we also found 22 BAs that constituted statistically significant connections in both samples. Within the left hemisphere, 11 (50.00%) of these were related to the P-FIT model (BAs 6, 7, 8, 9, 10, 21, 39, 40, 42, 46, 47) and two (9.09%) were not (BAs 4, 22). Within the right hemisphere, four (18.18%) were related to the P-FIT model (BAs 9, 32, 40, 46) and five (22.73%) were not (BAs 22, 42, 43, 44, 45).

Subsequent to examining the entire samples, we also conducted aforementioned analyses for male and female participants separately. Within both male subsamples, we did not observe a single statistically significant association between functional connectivity and matrix reasoning performance after applying correction for multiple comparisons. In contrast, we found 33 partial correlation coefficients that reached statistical significance in the female subsample of S498 (8.23%, $r = 0.18$–0.29) (Supplementary Fig. 5). As with the entire sample, the majority of connections was exclusively constituted by BAs from the P-FIT network (20 out of 33, 60.61%). Further, 13 connections included one BA from the P-FIT network and one unrelated BA (39.39%), while no connection was completely unrelated to the P-FIT network. The overall set of significant connections included 11 intrahemispheric connections in the left hemisphere (33.33%), seven intrahemispheric connections in the right hemisphere (21.21%), and 15 interhemispheric connections (45.45%) (Supplementary Fig. 6). Within the female subsample of S991, we identified 13 functional connections which exhibited statistically significant associations between functional connectivity and PMAT24 test scores (3.24%, $r = 0.14$–0.17) (Supplementary Fig. 7). We found seven of these connections to be entirely constituted by P-FIT areas (53.85%), three connections to be partly constituted by P-FIT areas (23.08%), and three connections to be constituted by BAs that were entirely unrelated to the P-FIT network (23.08%). In view of the general trajectories of these statically significant connections, we observed six intrahemispheric connections in the left hemisphere (46.15%), two intrahemispheric connections in the right hemisphere (15.38%), and five interhemispheric connections (38.46%) (Supplementary Fig. 8). Two of the 33 statistically significant connections in the female subsample of S498 were also present among the 13 connections in the female subsample of S991. One of them was an intrahemispheric connection already observed for the entire samples, namely that between left hemispheric BAs 8 and 47 (S498: $r = 0.18$, $p < .01$; S991: $r = 0.15$, $p < .001$). The other was an interhemispheric connection between BA 42 in the left and BA 22 in the right hemisphere (S498: $r = 0.19$, $p < .01$; S991: $r = 0.14$, $p < .001$). In addition, we also identified 12 BAs that constituted statistically significant connections in the female subsamples of S498 and S991. All of the six BAs within the left hemisphere (50.00%) were related to the P-FIT model (BAs 8, 10, 40, 42, 46, 47). Within the right hemisphere, three BAs (25.00%) were related to the P-FIT model (BAs 10, 40, 46) and three (25.00%) were not (BAs 22, 44, 45).

In order to further examine the five statistically significant connections which replicated across both samples, we conducted various multiple regression analyses. For the respective regression models, the normalized BOLD signal correlations exhibited by aforementioned five connections were used as independent variables. In the S498 sample (Supplementary Table 1), BOMAT test scores served as the dependent variable, whereas PMAT24 test scores were used as the dependent variable in the S991 sample (Supplementary Table 2). All following results refer to the adjusted R^2 of respective regression models. When utilizing data from the entire samples, the regression model of sample S498 was able to explain 4.60% of variance in matrix reasoning performance and that of sample S991 yielded 3.35% of explained variance. Both models were found to be highly significant ($p < .001$). Moreover, the functional connection between BA 46 in the left and BA 44 in the right hemisphere exhibited the highest unique contribution towards predicting matrix

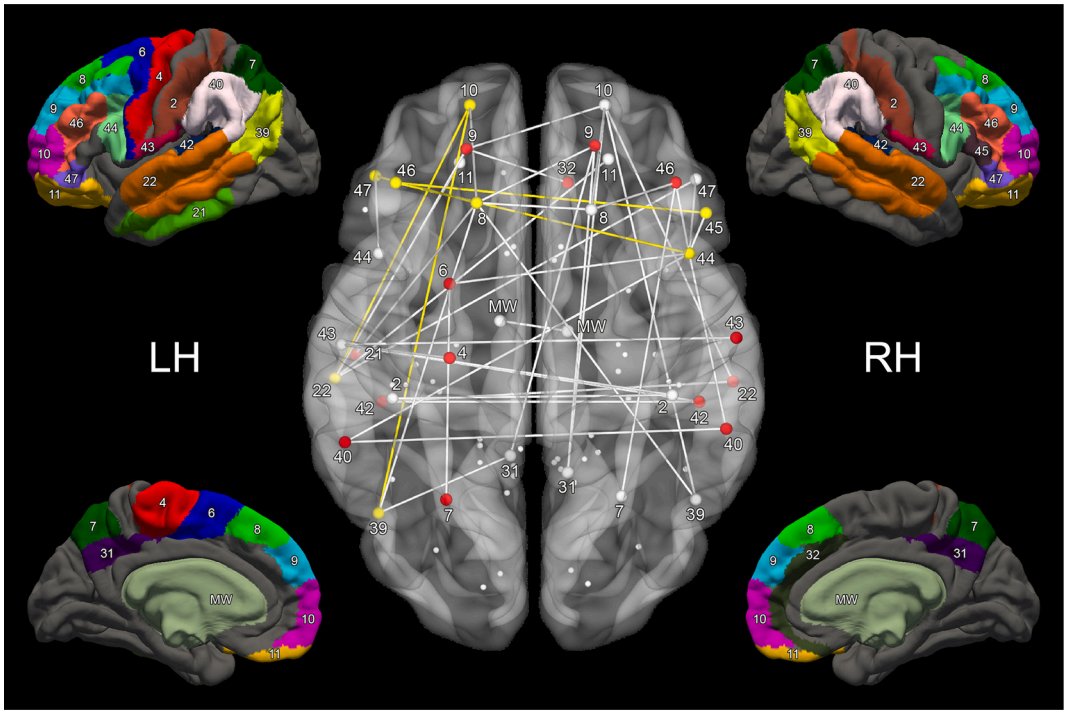

Fig. 5. Schematic depiction of functional connections showing statistically significant associations with matrix reasoning performance in sample S991. Brodmann areas included in the parcellation scheme used for this study are shown as white spheres within the semi-transparent MNI brain in the center. Functional connections exerting statistically significant correlations between their connectivity strength and matrix reasoning performance are shown as white lines. Spheres constituting statistically significant connections are slightly bigger than the rest and carry labels with the numbers of their corresponding Brodmann areas. Spheres and lines representing functional connections which replicated across both samples (S498 and S991) are depicted in yellow. Brodmann areas which were involved in statistically significant connections in both samples are represented by red spheres. All Brodmann areas constituting statistically significant connections are also shown as colored labels on four brain surfaces in the corners (lateral and medial views of the left and right hemispheres). (For interpretation of the references to colour in this figure legend, the reader is referred to the web version of this article.)

reasoning performance in both samples (S498: $\beta = 0.12$, $p < .05$; S991: $\beta = 0.16$, $p < .05$).

Subsequent to the analysis of the entire samples, we computed aforementioned models separately for both sexes using only data from the male and female subsamples, respectively. The model based on the male subsample of S498 explained less variance compared to the overall sample's model and did not reach statistical significance ($R^2_{adj} = 2.20\%$, $p = .066$). In contrast, explained variance was highest in the model based on the female subsample, which also turned out to be highly significant ($R^2_{adj} = 7.23\%$, $p < .001$). Results showed a similar pattern for the S991 sample. Here, both models reached statistical significance, but the male subsample's model ($R^2_{adj} = 1.96\%$, $p < .05$) explained less variance in matrix reasoning performance compared to the overall sample's model and the female subsample's model ($R^2_{adj} = 3.94\%$, $p < .001$).

In a last step, we computed all of the aforementioned regression models with randomly picked subsamples including only 75% of participants. For each of the entire samples as well as their male and female subsample's, we computed 10,000 iterations of the respective model and averaged relevant test statistics. In so doing, we found that mean explained variance was highest in regression models based on female subsamples (S498: $R^2_{adj\_mean} = 7.21\%$; S991: $R^2_{adj\_mean} = 3.99\%$), followed by models based on entire samples (S498: $R^2_{adj\_mean} = 4.59\%$; S991: $R^2_{adj\_mean} = 3.36\%$), followed by models based on male subsamples (S498: $R^2_{adj\_mean} = 2.24\%$; S991: $R^2_{adj\_mean} = 1.96\%$). Additional test statistics, such as the range of explained variance or the ratio of statistically significant iterations, are summarized in Supplementary Table 3.

4. Discussion

The primary goal of this study was to investigate the relationship between matrix reasoning performance and functional connectivity, especially with regard to BAs included in the P-FIT network. Our first hypothesis suggested that higher functional coherence at rest, quantified as normalized BOLD signal correlations between BAs, would lead to higher performance on matrix reasoning tests. The parcellation scheme that was utilized for this study delineates a total of 82 BAs for the whole brain with less than half of them, namely 31 BAs, constituting the P-FIT network. Given this ratio and assuming a completely random distribution of statistically significant connections, one would expect 14.00% of these connections to be exclusively constituted by P-FIT BAs, 38.39% of connections to be completely unrelated to the P-FIT network, and 47.61% of connections to involve one P-FIT BA and one unrelated region. However, our data revealed a deviating pattern with a strong emphasis on the involvement of P-FIT BAs. For sample S498, we identified 31 connections that reached statistical significance after correcting for multiple comparisons. Respective connections were exclusively constituted by BAs from the P-FIT network in 20 out of 31 cases (64.52%), almost five times the expected ratio. Consequentially, statistically significant connections that were partially constituted by P-FIT BAs (9 out of 31 cases, 29.03%) or did not have any relations to the P-FIT network (2 out of 31 cases, 6.45%) fell short of their expected ratios. Comparable results were revealed by analyzing data from sample S991. In total, we identified 43 statistically significant connections, of which the majority, namely 17 connections or 39.53%, turned out to be constituted by P-FIT BAs exclusively. As with sample S498, connections that were partially constituted by P-FIT BAs (15 out of 43 cases, 34.88%) or completely unrelated to the P-FIT network (11 out of 43 cases, 25.58%) did not reach their expected ratios. Based on these findings

from two large and independent datasets, it is fair to say that our first hypothesis could be confirmed. In both samples, statistically significant associations between functional connectivity and matrix reasoning performance were predominantly exhibited by connections between BAs from the P-FIT network, while connections unrelated to the model were of less importance.

Interestingly, our separate analyses of male and female subsamples revealed patterns similar to the entire S498 and S991 samples but only in the female subsamples. While we did not observe a single statistically significant result within both male subsamples, the female subsample of S498 showed 20 connections (60.61%) that were exclusively and 13 connections (39.39%) that were partially constituted by P-FIT BAs. Moreover, none of the connections was completely unrelated to the P-FIT network. For the female subsample of S991, we found seven connections (53.85%) that were exclusively and three connections (23.08%) that were partially constituted by P-FIT BAs as well as three connections (23.08%) completely unrelated to the P-FIT network. We did not expect the aforementioned shift towards a more pronounced involvement of P-FIT connections to be sex-specific. However, this observation is well in line with previous reports on divergent neural correlates of matrix reasoning performance in male and female individuals. More specifically, Genc et al. (2019) found cortex volume to be the best predictor of BOMAT test scores in male individuals, whereas a graph theoretical measure of functional resting-state connectivity turned out to be the best predictor in female individuals. On the population level, men and women do not show substantial differences with regard to their intelligence. However, they can vary considerably in particular aspects of their brain anatomy. For example, it is well-known that brain volume, which has consistently been reported to be positively associated with intelligence (Pietschnig et al., 2015), is 10% larger in men compared to women (Ruigrok et al., 2014). Therefore, it is conceivable that female individuals draw on different aspects of their neural substrate, e.g. functional connectivity, in order to achieve comparable levels of cognitive performance.

In view of the replicability of our results, it is important to note that there were five statistically significant connections which were present in the S498 as well as the S991 sample. Two of these connections were entirely constituted by P-FIT areas (BAs 8, 10, 39, and 47 in the left hemisphere) and the remaining three were comprised of a combination between P-FIT areas (BAs 10 and 46 in the left hemisphere) and areas unrelated to the P-FIT network (BA 22 in the left and BAs 44 and 45 in the right hemisphere). In the following, we would like to elaborate on these particular BAs and the cognitive functions usually associated with them. BA 8 is located anterior to the premotor cortex an includes the frontal eye fields, which have been related to visual attention and eye movements (Schall, 2004). Despite being situated in the frontal cortex, which is mainly associated with high-level information processing, BA 8 has also been shown to be a quickly activated multimodal region that belongs to a network of low-level neocortical sensory areas (Kirchner, Barbeau, Thorpe, Régis, & Liégeois-Chauvel, 2009). Given its involvement in visual information processing, functional connections emanating from BA 8 might be of importance when working on visually presented problems such as matrix reasoning items. In addition to that, there is evidence that functional activation of BA 8 is tied to the experience of uncertainty (Volz, Schubotz, & von Cramon, 2005), which is likely to occur during a matrix reasoning test, especially when working on particularly difficult items. BA 10 is the anterior-most portion of the prefrontal cortex. In the original meta-analysis by Jung and Haier (2007), this area takes a special place in that it approaches a comparatively high level of convergence across studies in which structural properties were related to intelligence. Our results show that matrix reasoning performance is associated with functional connectivity between BAs 10 and 39 but also between BAs 10 and 22. In case of the latter pathway, there is histological evidence from a study by Petrides and Pandya (2007), in which it was shown that the rostral prefrontal cortex of macaque monkeys exhibits fiber connections to the superior temporal gyrus. With regard to the function of BA 10, it has been stated that "hemodynamic changes in area 10 can occur during virtually any kind of cognitive paradigm, from the simplest conditioning paradigms to the most complex tests" (Burgess, Dumontheil, & Gilbert, 2007). Hence, BA 10 is considered to be primarily involved in domain-general functions such as working memory (Gilbert et al., 2006) or cognitive branching (Koechlin & Hyafil, 2007). Moreover, it has also been hypothesized that BA 10 supports the integration of diverse information by attending to both environmental stimuli and self-generated mental representations, i.e. thoughts (Burgess et al., 2007). BA 39 encompasses the angular gyrus and has been proposed to form an extended Wernicke's area together with BAs 20, 37, and 38 (Ardila, Bernal, & Rosselli, 2016). As part of this language association network, BA 39 is not involved in core processes of language perception but believed to serve additional functions such as associating words with other information. In line with this, BA 39 is known to be significantly abnormal in dyslexic dysfunction (Rae et al., 1998; Rumsey et al., 1992). Just like BA 10, BA 39 is also among the few brain areas in Jung and Haier (2007), which reach a high level of convergence across studies on structural correlates of intelligence. BAs 46 and 47 are both situated on the lateral frontal cortex. Similar to BAs 10 and 39, BA 46 also approached a high level of convergence across studies from Jung and Haier (2007), but in this case with regard to intelligence correlates identified by means of positron emission tomography. Complementary to BA 39 supporting the perception of language, BAs 46 and 47 are hypothesized to be part of a complex frontal-subcortical circuit involved in language production and grammar known as Broca's complex (Ardila et al., 2016). Further, BAs 44 and 45 are supposed to constitute the core of this complex. Importantly, given that language production is usually lateralized to the left hemisphere, especially in right-handed individuals (Ocklenburg, Beste, Arning, Peterburs, & Guentuerkuen, 2014), it is somewhat surprising that our analyses yielded significant results for left-hemispheric BAs 46 and 47 but right-hemispheric BAs 44 and 45. As mentioned above, we found BAs 10 and 22 to exhibit a statistically significant connection. BA 22 is located in the posterior segment of superior temporal gyrus. In the left hemisphere, it constitutes a core Wernicke's area together with BAs 21, 41, and 42 (Ardila et al., 2016). Taken together, these results indicate that the association between matrix reasoning performance and functional connectivity is strongly affected by areas involved in language processing (BAs 22, 39, 44, 45, 46, 47). Language has been considered to be an important cognitive tool for reasoning (Varley, 2007). On the one hand, it provides a set of symbols that permits the encapsulation and manipulation of abstract notions. On the other hand, its grammatical mechanisms allow for relationships between entities to be captured. Furthermore, language is crucial for inner speech, which can guide the reasoning process, e.g. by breaking down a complex problem into a series of sub-steps. Based on these assumptions, the functional connectivity patterns observed in our results might represent the following mechanisms potentially underlying matrix reasoning. The frontal eye fields encompassed by BA 8 are likely to support the extraction of sensory information from a matrix reasoning problem by initiating saccadic eye movements and engaging in early visual processing. Respective information might constantly be forwarded to language-related areas (BAs 22, 39, 44, 45, 46, 47), in which a verbalized mental representation of the problem is formed and used to come up with an adequate solution. Moreover, it is conceivable that this process of integrating external visual information and internal mental representations is primarily guided by BA 10. By subjecting the functional connections comprised in this model to multiple regression analysis, we found them to explain about 4% to 6% of variance in matrix reasoning performance, depending on the sample we used. In neuroscientific intelligence research, explained variance typically falls into this order of magnitude, given that the association between intelligence and its neural correlates is characterized by supervenience (many-to-one) rather than isomorphism (one-to-one) (Kievit et al., 2011; Ritchie et al., 2015). Furthermore, multiple regression analysis revealed that the

predictive power of our model was higher and more stable for female compared to male individuals. As mentioned above, this finding is well in line with previous research showing a more pronounced relationship between intelligence and functional correlates for female brains and a stronger influence of structural correlates for male brains (Genc et al., 2019).

For the P-FIT model a serial flow of information is assumed with cognitive processing proceeding from the occipital and temporal lobes to parietal, frontal, and cingulate regions in consecutive order. Thus, we hypothesized that functional connections, exhibiting statistically significant associations between their connection strength and matrix reasoning performance, should mainly comply to this pattern. Among the five functional connections which replicated across both samples, we observed one temporal-frontal connection (BA 22 to BA 10), one parietal-frontal connection (BA 39 to BA 10), and one frontal-frontal connection (BAs 8 to BA 47), all of them in the left hemisphere, as well as two interhemispheric frontal-frontal connections (BA 46 to BA 44 and BA 46 to BA 47). Since the original P-FIT model does not make any assumptions with regard to intra- or interhemispherically organized connections within the same lobe, we do not consider respective connections to be a violation of the serial flow model. Further, the parietal-frontal connection between BAs 39 and 10 in the left hemisphere matches the model proposed by P-FIT. In contrast, the temporal-frontal connection between BAs 22 and 10 in the left hemisphere is not in line with the serial flow model in that it bypasses information exchange with parietal areas. Importantly, given that matrix reasoning usually revolves around visually presented information, the involvement of BA 22 is unlikely to stem from the early processing of external auditory stimuli. As mentioned above, we consider it to be more feasible that BA 22 is part of a language-related network, which enables an individual to use inner speech for the purpose of problem solving. In general, our results favor a more parallel flow of information with BA 10 utilizing visual information provided by BA 8 to constantly update a verbalized mental representation used by language-related areas (BAs 22, 39, 44, 45, 46, 47). In return, inner speech emerging from the language-related areas might guide the extraction of additional visual information by sending feedback to BA 8. It has to be noted that this model is based on fMRI data that were recorded with participants at rest instead of actively solving matrix reasoning problems. Hence, it is possible that task-based data might yield slightly different associations between matrix reasoning performance and functional connectivity patterns. In addition to that, the functional connections yielded by our analyses are based on BOLD signal correlations between whole cortical areas. Therefore, they lack information about directionality, which makes it hard to interpret respective data with regard to flow of information. A possible solution to this problem is to employ fMRI data recorded at a higher magnetic field strength, e.g. 7 Tesla. In so doing, one can assess images with a considerably higher spatial resolution and obtain information about hemodynamic changes at the level of individual cortical layers. According to the canonical model of cortical layer connectivity, feedforward activity is found in middle layers, whereas feedback activity is located in superficial and/or deep layers, depending on the brain region under investigation (Finn, Huber, Jangraw, Molfese, & Bandettini, 2019; Markov et al., 2013; Sharoh et al., 2019). An even more sophisticated approach towards the disentanglement of feedforward and feedback information flow involves the analysis of simultaneously recorded data from fMRI and electroencephalography (Scheeringa, Koopmans, van Mourik, Jensen, & Norris, 2016). In combination, these measures would permit direct testing of the serial flow of information model as proposed by Jung and Haier (2007).

Our third hypothesis suggested that the association between functional connectivity and matrix reasoning performance is represented by both positive and negative correlation coefficients. Although we initially observed both negative and positive associations, our third hypothesis had to be rejected since none of the negative correlations survived correction for multiple comparisons. All of the statistically significant associations that remained, 31 in the S498 sample and 43 in the S991 sample, were positive. This absence of negative correlations is not in line with previous studies, in which inverse relations between measures of functional connectivity and intelligence have been reported. For example, Song et al. (2008) observed negative correlations between intelligence and functional connectivity exhibited by connections linking the left dorsolateral prefrontal cortex to BA 10 of both hemispheres. However, when the authors subjected all statistically significant functional connections to a stepwise linear analysis, none of the inverse associations were retained in the resulting model. Another study by Hilger et al. (2017b), investigated the relationship between brain's modular organization and intelligence. In view of between-module connectivity, the authors observed negative associations for node clusters in medial superior frontal gyrus, left inferior parietal lobule, and bilateral temporo-parietal junction. Furthermore, they found intelligence and within-module connectivity to be negatively associated for node clusters in right anterior insula, bilateral precentral gyrus, bilateral hippocampi, and subcortically in the left caudate nucleus. According to the authors, nodes exhibiting negative associations between intelligence and between-module connectivity might possess a vital role in shielding ongoing cognitive processes from interfering noise. Similarly, nodes showing negative associations between intelligence and within-module connectivity might benefit from a more independent and shielded position within their own functional module. Generally speaking, negative correlations between measures of cognitive performance and functional connectivity are likely to be found in brain areas characterized by segregated information processing, i.e. increasing signal-to-noise ratio by avoiding unnecessary crosstalk and the exchange of irrelevant information (Cohen & D'Esposito, 2016). As opposed to aforementioned research, our analyses did not yield any results in support of such mechanisms. These inconsistencies between studies might be attributed to differences in the analytical approach (whole-brain vs. seed-based, individual BOLD signal correlations vs. graph metrics), choice of behavioral variables (matrix reasoning performance vs. general intelligence), or size and composition of samples. Notwithstanding the above, it might be interesting to see if the use of task-based fMRI data, capturing the brain while engaging in information processing, would yield substantially different results compared to fMRI resting-state data.

Within both samples, the vast majority of functional connections, including those theoretically nominated by the P-FIT model, did not exhibit statistically significant associations between their connectivity strength and matrix reasoning performance. To recapitulate, our analyses started out with functional connectivity matrices holding information about 3321 individual connections in the form of normalized BOLD signal correlations. In order to remove spurious connections, we computed pruned versions of these matrices containing merely 401 functional connections. Among these, 121 were constituted entirely by areas from the P-FIT network, 160 were partially built by P-FIT areas, and 120 were completely unrelated to P-FIT. Out of the 281 functional connections involving at least one P-FIT area, only 29 connections (10.32%) from sample S498 exhibited statistically significant associations between their connectivity strength and matrix reasoning performance. For sample S991, we observed 32 (11.39%) such connections. In order to arrive at an exact number of functional connections theoretically nominated by the P-FIT model, one would have to consider only those connections conforming to the serial flow of information model. However, even when taking these restrictions into account the ratio between observed and potential P-FIT connections would remain fairly low. Hence, the question arises if the original version of the P-FIT network should be pruned based on our data. In this regard, it has to be noted that the research question tackled in the meta-analysis conducted by Jung and Haier (2007) is slightly different from that of our work. While the P-FIT model nominates brain areas whose properties, such as task-based functional activation, have been consistently associated with intelligence, our study is focused on functional brain connections and how their strength is related to matrix reasoning performance. In our

opinion, it is quite possible that a particular brain area is strongly involved in mental problem solving even though it does not show intelligence-related functional connectivity, neither during a task nor at rest.

When comparing the results obtained from both datasets utilized for this study, it has to be noted that the statistically significant connections identified for sample S498 do not match exactly those in sample S991. In total, we identified 31 statistically significant connections in the S498 sample and 43 connections in the S991 sample. However, only five of these connections, about 12–16%, replicated across both samples. Although the replication of results across multiple datasets is considered desirable, it has to be understood that such efforts are to some extent limited by the substantial differences between datasets. The two samples used for the study at hand differed with regard to their matrix reasoning tests, sample sizes, image acquisition protocols, and preprocessing pipelines. For example, the "advanced short version" of BOMAT, which was used for our data acquisition, has more items compared to PMAT24 (29 instead of 24) and was designed high discriminatory power in mind, especially in samples with generally high intellectual abilities, thus avoiding possible ceiling effects. Moreover, our behavioral data acquisition was solely focused on matrix reasoning performance, whereas the Human Connectome Project conducted the PMAT24 along with a large variety of other tests unrelated to matrix reasoning performance or other forms of intelligence. Hence, it is possible that BOMAT test scores provide a slightly more precise estimate of matrix reasoning performance compared to PMAT24 test scores. However, it has to be noted that the S991 sample comprised about two times as many subjects as the S498 sample. Therefore, it is also conceivable that potential noise within the behavioral data was mitigated more strongly in the S991 sample due to its larger size. Further differences between both samples can be identified in the acquisition of fMRI data. Whereas participants from the S498 were told to keep their eyes closed during resting-state scans, participants from the S991 sample were instructed to keep their eyes open. Effects caused by such differences in instruction have been found to be relatively small but significant (Patriat et al., 2013). In our data, functional connections involving areas from the primary visual cortex did not show any significant associations with matrix reasoning performance in both samples. Likewise, both samples exhibited statistically significant functional connections emanating from BA 8, which is involved in visual processing since it contains the frontal eye fields. Hence, albeit different methods were used to acquire resting-state data, instructing participants to keep their eyes closed or open did not cause substantially different results between both samples. In addition to said differences in instruction, the acquisition time of resting-state data was 7 min in the S498 sample and 30 min in the S991 sample. Birn et al. (2013) came to the conclusion that the intersession reliability of functional connectivity data is significantly increased by acquisition time, but only if all functional connections within a network of interest are considered. In pruned networks, from which all spurious connections that failed to reach statistical significance are removed, the beneficial effects of longer acquisition times begin to plateau at around 9 min. In following a pruning approach for the analysis of our fMRI data, we aimed to diminish the differences in reliability between both samples as much as possible. Considering these and other marked differences between both samples, it is obvious why we did not find results from sample S498 to perfectly match those yielded by sample S991. However, this also renders the findings replicating across both samples to be even robust.

In conclusion, by analyzing data from two independent datasets comprising a total of 1489 healthy individuals, we were able to identify several functional connections, all of them related to the P-FIT network, whose connectivity strength at rest was significantly associated with matrix reasoning performance. In previous research, the brain areas constituting respective connections have been shown to be primarily involved in language processing. Hence, it is conceivable that our results reflect the importance of inner speech for solving matrix reasoning tasks or even other intelligence-related problems. It might be interesting for future research to take up the approach of our study, namely to examine intelligence-related correlates on the level of individual brain network connections, and extend it in various ways. For example, one might employ other measures of intellectual performance, such as general intelligence, or utilize task-based fMRI data recorded while subjects are actively working on cognitively demanding problems. In view of functional network construction, it might be beneficial to delineate brain images into individual nodes based on functional properties instead of anatomical locations or topographic conformations, e.g. by means of hyperalignment (Feilong, Nastase, Guntupalli, & Haxby, 2018). Furthermore, structural metrics obtained via diffusion-weighted imaging might be used as another way of quantifying network connectivity. Lastly, one might conduct simultaneous recordings of fMRI and EGG data at ultra-high magnetic field strength in order to reveal the flow of information along functional connections relevant for interindividual differences in intellectual performance.

Funding

This work was supported by the Deutsche Forschungsgemeinschaft (grant numbers GU 227/16-1, GE 2777/2-1, Sonderforschungsbereich 1280 project A03) and the Mercator Research Center Ruhr (MERCUR) (grant number An-2015-0044). Data were provided in part by the Human Connectome Project, WU-Minn Consortium (Principal Investigators: David Van Essen and Kamil Ugurbil; 1U54MH091657) funded by the 16 NIH Institutes and Centers that support the NIH Blueprint for Neuroscience Research; and by the McDonnell Center for Systems Neuroscience at Washington University.

Author contributions

E.G. conceived the project and supervised the experiments. C.F., O. G., R.J., and E.G. designed the project. C.F., C.S., and P.F. collected the data. C.F., and E.G. analyzed the data. C.F. and E.G. wrote the manuscript. All authors discussed the results and edited the manuscript.

Acknowledgements

The authors thank all student assistants for their support during the behavioral measurements. Further, the authors thank Lara Schlaffke and PHILIPS Germany (Burkhard Mädler) for their scientific support with the MRI measurements as well as Tobias Otto for his technical support.

Appendix A. Supplementary data

Supplementary data to this article can be found online at https://doi.org/10.1016/j.intell.2021.101545.

References

Amunts, K., Jäncke, L., Mohlberg, H., Steinmetz, H., & Zilles, K. (2000). Interhemispheric asymmetry of the human motor cortex related to handedness and gender. *Neuropsychologia, 38*(3), 304–312.

Amunts, K., Schlaug, G., Schleicher, A., Steinmetz, H., Dabringhaus, A., Roland, P. E., & Zilles, K. (1996). Asymmetry in the human motor cortex and handedness. *Neuroimage, 4*(3), 216–222.

Ardila, A., Bernal, B., & Rosselli, M. (2016). How localized are language brain areas? A review of Brodmann areas involvement in oral language. *Archives of Clinical Neuropsychology, 31*(1), 112–122.

Avery, E. W., Yoo, K., Rosenberg, M. D., Greene, A. S., Gao, S., Na, D. L., … Chun, M. M. (2020). Distributed patterns of functional connectivity predict working memory performance in novel healthy and memory-impaired individuals. *Journal of Cognitive Neuroscience, 32*(2), 241–255.

Basten, U., Hilger, K., & Fiebach, C. J. (2015). Where smart brains are different: A quantitative meta-analysis of functional and structural brain imaging studies on intelligence. *Intelligence, 51*, 10–27.

Benjamini, Y., & Hochberg, Y. (1995). Controlling the false discovery rate - a practical and powerful approach to multiple testing. *Journal of the Royal Statistical Society, Series B (Statistical Methodology), 57*(1), 289–300.

Birn, R. M., Molloy, E. K., Patriat, R., Parker, T., Meier, T. B., Kirk, G. R., … Prabhakaran, V. (2013). The effect of scan length on the reliability of resting-state fMRI connectivity estimates. *Neuroimage, 83*, 550–558.
Brodmann, K. (1909). *Vergleichende Lokalisationslehre der Grosshirnrinde in ihren Prinzipien dargestellt auf Grund des Zellenbaues*. Johann Ambrosius Barth Verlag.
Burgess, P. W., Dumontheil, I., & Gilbert, S. J. (2007). The gateway hypothesis of rostral prefrontal cortex (area 10) function. *Trends in Cognitive Sciences, 11*(7), 290–298.
Cohen, J. R., & D'Esposito, M. (2016). The segregation and integration of distinct brain networks and their relationship to cognition. *Journal of Neuroscience, 36*(48), 12083–12094.
Dale, A. M., Fischl, B., & Sereno, M. I. (1999). Cortical surface-based analysis. I. Segmentation and surface reconstruction. *Neuroimage, 9*(2), 179–194.
Deary, I. J. (2012). Intelligence. *Annual Review of Psychology, 63*, 453–482.
Deary, I. J., Penke, L., & Johnson, W. (2010). The neuroscience of human intelligence differences. *Nature Reviews Neuroscience, 11*(3), 201–211.
Dubois, J., Galdi, P., Paul, L. K., & Adolphs, R. (2018). A distributed brain network predicts general intelligence from resting-state human neuroimaging data. *Philosophical Transactions of the Royal Society, B: Biological Sciences, 373*(1756).
Ezaki, T., Fonseca Dos Reis, E., Watanabe, T., Sakaki, M., & Masuda, N. (2020). Closer to critical resting-state neural dynamics in individuals with higher fluid intelligence. *Communications Biology, 3*(1), 52.
Faul, F., Erdfelder, E., Buchner, A., & Lang, A. G. (2009). Statistical power analyses using G*Power 3.1: Tests for correlation and regression analyses. *Behavior Research Methods, 41*(4), 1149–1160.
Feilong, M., Nastase, S. A., Guntupalli, J. S., & Haxby, J. V. (2018). Reliable individual differences in fine-grained cortical functional architecture. *Neuroimage, 183*, 375–386.
Finn, E. S., Huber, L., Jangraw, D. C., Molfese, P. J., & Bandettini, P. A. (2019). Layer-dependent activity in human prefrontal cortex during working memory. *Nature Neuroscience, 22*(10), 1687–1695.
Finn, E. S., Shen, X. L., Scheinost, D., Rosenberg, M. D., Huang, J., Chun, M. M., … Constable, R. T. (2015). Functional connectome fingerprinting: Identifying individuals using patterns of brain connectivity. *Nature Neuroscience, 18*(11), 1664–1671.
Fischl, B., Sereno, M. I., & Dale, A. M. (1999). Cortical surface-based analysis. II: Inflation, flattening, and a surface-based coordinate system. *Neuroimage, 9*(2), 195–207.
Fisher, R. A. (1921). On the probable error of a coefficient of correlation deduced from a small sample. *Metron, 1*, 3–32.
Fox, M. D., & Raichle, M. E. (2007). Spontaneous fluctuations in brain activity observed with functional magnetic resonance imaging. *Nature Reviews Neuroscience, 8*(9), 700–711.
Frith, E., Elbich, D. B., Christensen, A. P., Rosenberg, M. D., Chen, Q., Kane, M. J., … Beaty, R. E. (2021). Intelligence and creativity share a common cognitive and neural basis. *Journal of Experimental Psychology: General, 150*(4), 609–632.
Genc, E., Fraenz, C., Schlueter, C., Friedrich, P., Hossiep, R., Voelkle, M. C., … Jung, R. E. (2018). Diffusion markers of dendritic density and arborization in gray matter predict differences in intelligence. *Nature Communications, 9*(1), 1–11.
Genc, E., Fraenz, C., Schlueter, C., Friedrich, P., Voelkle, M. C., Hossiep, R., & Guentuerkuen, O. (2019). The neural architecture of general knowledge. *European Journal of Personality, 33*(5), 589–605.
Genc, E., Schoelvinck, M. L., Bergmann, J., Singer, W., & Kohler, A. (2016). Functional connectivity patterns of visual cortex reflect its anatomical organization. *Cerebral Cortex, 26*(9), 3719–3731.
Gilbert, S. J., Spengler, S., Simons, J. S., Steele, J. D., Lawrie, S. M., Frith, C. D., & Burgess, P. W. (2006). Functional specialization within rostral prefrontal cortex (area 10): A meta-analysis. *Journal of Cognitive Neuroscience, 18*(6), 932–948.
Glasser, M. F., Coalson, T. S., Robinson, E. C., Hacker, C. D., Harwell, J., Yacoub, E., … Van Essen, D. C. (2016). A multi-modal parcellation of human cerebral cortex. *Nature, 536*(7615), 171–178.
Glasser, M. F., Sotiropoulos, S. N., Wilson, J. A., Coalson, T. S., Fischl, B., Andersson, J. L., … Jenkinson, M. (2013). The minimal preprocessing pipelines for the Human Connectome Project. *Neuroimage, 80*(1), 105–124.
Haier, R. J., Siegel, B. V., Nuechterlein, K. H., Hazlett, E., Wu, J. C., Paek, J., … Buchsbaum, M. S. (1988). Cortical glucose metabolic-rate correlates of abstract reasoning and attention studied with positron emission tomography. *Intelligence, 12*(2), 199–217.
van den Heuvel, M. P., Stam, C. J., Kahn, R. S., & Hulshoff Pol, H. E. (2009). Efficiency of functional brain networks and intellectual performance. *Journal of Neuroscience, 29*(23), 7619–7624.
Hilger, K., Ekman, M., Fiebach, C. J., & Basten, U. (2017a). Efficient hubs in the intelligent brain: Nodal efficiency of hub regions in the salience network is associated with general intelligence. *Intelligence, 60*, 10–25.
Hilger, K., Ekman, M., Fiebach, C. J., & Basten, U. (2017b). Intelligence is associated with the modular structure of intrinsic brain networks. *Scientific Reports, 7*(1), 1–12.
Hossiep, R., Hasella, M., & Turck, D. (2001). *BOMAT - Advanced-short version: Bochumer Matrizentest*. Hogrefe.
Jung, R. E., & Haier, R. J. (2007). The Parieto-Frontal Integration Theory (P-FIT) of intelligence: Converging neuroimaging evidence. *Behavioral and Brain Sciences, 30*(2), 135–154.
Karama, S., Colom, R., Johnson, W., Deary, I. J., Haier, R., Waber, D. P., … Evans, A. C. (2011). Cortical thickness correlates of specific cognitive performance accounted for by the general factor of intelligence in healthy children aged 6 to 18. *Neuroimage, 55*(4), 1443–1453.
Kievit, R. A., Romeijn, J. W., Waldorp, L. J., Wicherts, J. M., Scholte, H. S., & Borsboom, D. (2011). Mind the gap: A psychometric approach to the reduction problem. *Psychological Inquiry, 22*(2), 67–87.
Kirchner, H., Barbeau, E. J., Thorpe, S. J., Régis, J., & Liégeois-Chauvel, C. (2009). Ultra-rapid sensory responses in the human frontal eye field region. *Journal of Neuroscience, 29*(23), 7599–7606.
Klingberg, T. (2010). Training and plasticity of working memory. *Trends in Cognitive Sciences, 14*(7), 317–324.
Koechlin, E., & Hyafil, A. (2007). Anterior prefrontal function and the limits of human decision-making. *Science, 318*(5850), 594–598.
Kruschwitz, J. D., Waller, L., Daedelow, L. S., Walter, H., & Veer, I. M. (2018). General, crystallized and fluid intelligence are not associated with functional global network efficiency: A replication study with the human connectome project 1200 data set. *Neuroimage, 171*, 323–331.
Li, Y., Liu, Y., Li, J., Qin, W., Li, K., Yu, C., & Jiang, T. (2009). Brain anatomical network and intelligence. *PLoS Computational Biology, 5*(5), 1–17.
Markov, N. T., Ercsey-Ravasz, M., Van Essen, D. C., Knoblauch, K., Toroczkai, Z., & Kennedy, H. (2013). Cortical high-density counterstream architectures. *Science, 342*(6158).
McDaniel, M. A. (2005). Big-brained people are smarter: A meta-analysis of the relationship between in vivo brain volume and intelligence. *Intelligence, 33*(4), 337–346.
Moore, T. M., Reise, S. P., Gur, R. E., Hakonarson, H., & Gur, R. C. (2015). Psychometric properties of the Penn Computerized Neurocognitive Battery. *Neuropsychology, 29*(2), 235–246.
Narr, K. L., Woods, R. P., Thompson, P. M., Szeszko, P., Robinson, D., Dimtcheva, T., … Bilder, R. M. (2007). Relationships between IQ and regional cortical gray matter thickness in healthy adults. *Cerebral Cortex, 17*(9), 2163–2171.
Neubauer, A., & Fink, A. (2009). Intelligence and neural efficiency: Measures of brain activation versus measures of functional connectivity in the brain. *Intelligence, 37*(2), 223–229.
Ocklenburg, S., Beste, C., Arning, L., Peterburs, J., & Guentuerkuen, O. (2014). The ontogenesis of language lateralization and its relation to handedness. *Neuroscience and Biobehavioral Reviews, 43*, 191–198.
Oelhafen, S., Nikolaidis, A., Padovani, T., Blaser, D., Koenig, T., & Perrig, W. J. (2013). Increased parietal activity after training of interference control. *Neuropsychologia, 51*(13), 2781–2790.
Oldfield, R. C. (1971). The assessment and analysis of handedness: The Edinburgh inventory. *Neuropsychologia, 9*(1), 97–113.
Patriat, R., Molloy, E. K., Meier, T. B., Kirk, G. R., Nair, V. A., Meyerand, M. E., … Birn, R. M. (2013). The effect of resting condition on resting-state fMRI reliability and consistency: A comparison between resting with eyes open, closed, and fixated. *Neuroimage, 78*, 463–473.
Penke, L., Maniega, S. M., Bastin, M. E., Hernandez, M. C. V., Murray, C., Royle, N. A., … Deary, I. J. (2012). Brain white matter tract integrity as a neural foundation for general intelligence. *Molecular Psychiatry, 17*(10), 1026–1030.
Petrides, M., & Pandya, D. N. (2007). Efferent association pathways from the rostral prefrontal cortex in the macaque monkey. *Journal of Neuroscience, 27*(43), 11573–11586.
Pietschnig, J., Penke, L., Wicherts, J. M., Zeiler, M., & Voracek, M. (2015). Meta-analysis of associations between human brain volume and intelligence differences: How strong are they and what do they mean? *Neuroscience and Biobehavioral Reviews, 57*, 411–432.
Power, J. D., Cohen, A. L., Nelson, S. M., Wig, G. S., Barnes, K. A., Church, J. A., … Petersen, S. E. (2011). Functional network organization of the human brain. *Neuron, 72*(4), 665–678.
Rae, C., Lee, M. A., Dixon, R. M., Blamire, A. M., Thompson, C. H., Styles, P., … Stein, J. F. (1998). Metabolic abnormalities in developmental dyslexia detected by 1H magnetic resonance spectroscopy. *The Lancet, 351*(9119), 1849–1852.
Raven, J., Raven, J. C., & Court, J. H. (2003). *Manual for Raven's progressive matrices and vocabulary scales. Section 1: General overview*. Harcourt Assessment.
Raymond, M., & Pontier, D. (2004). Is there geographical variation in human handedness? *Laterality, 9*(1), 35–51.
Ritchie, S. J., Booth, T., Valdes Hernandez, M. D., Corley, J., Maniega, S. M., Gow, A. J., … Deary, I. J. (2015). Beyond a bigger brain: Multivariable structural brain imaging and intelligence. *Intelligence, 51*, 47–56.
Ruigrok, A. N., Salimi-Khorshidi, G., Lai, M. C., Baron-Cohen, S., Lombardo, M. V., Tait, R. J., & Suckling, J. (2014). A meta-analysis of sex differences in human brain structure. *Neuroscience and Biobehavioral Reviews, 39*, 34–50.
Rumsey, J. M., Andreason, P., Zametkin, A. J., Aquino, T., King, A. C., Hamburger, S. D., … Cohen, R. M. (1992). Failure to activate the left temporoparietal cortex in dyslexia: An oxygen 15 positron emission tomographic study. *Archives of Neurology, 49*(5), 527–534.
Santarnecchi, E., Emmendorfer, A., & Pascual-Leone, A. (2017). Dissecting the parieto-frontal correlates of fluid intelligence: A comprehensive ALE meta-analysis study. *Intelligence, 63*, 9–28.
Santarnecchi, E., Emmendorfer, A., Tadayon, S., Rossi, S., Rossi, A., & Pascual-Leone, A. (2017). Network connectivity correlates of variability in fluid intelligence performance. *Intelligence, 65*, 35–47.
Schall, J. D. (2004). On the role of frontal eye field in guiding attention and saccades. *Vision Research, 44*(12), 1453–1467.
Scheeringa, R., Koopmans, P. J., van Mourik, T., Jensen, O., & Norris, D. G. (2016). The relationship between oscillatory EEG activity and the laminar-specific BOLD signal. *Proceedings of the National Academy of Sciences, 113*(24), 6761–6766.
Sharoh, D., van Mourik, T., Bains, L. J., Segaert, K., Weber, K., Hagoort, P., & Norris, D. G. (2019). Laminar specific fMRI reveals directed interactions in

distributed networks during language processing. *Proceedings of the National Academy of Sciences, 116*(42), 21185–21190.
Shen, X., Tokoglu, F., Papademetris, X., & Constable, R. T. (2013). Groupwise whole-brain parcellation from resting-state fMRI data for network node identification. *Neuroimage, 82*, 403–415.
Smith, S. M., Beckmann, C. F., Andersson, J., Auerbach, E. J., Bijsterbosch, J., Douaud, G., … Glasser, M. F. (2013). Resting-state fMRI in the Human Connectome project. *Neuroimage, 80*, 144–168.
Song, M., Zhou, Y., Li, J., Liu, Y., Tian, L. X., Yu, C., & Jiang, T. (2008). Brain spontaneous functional connectivity and intelligence. *Neuroimage, 41*(3), 1168–1176.
Spearman, C. (1904). "General intelligence" objectively determined and measured. *The American Journal of Psychology, 15*(2), 201–292.
Tavor, I., Jones, O. P., Mars, R. B., Smith, S. M., Behrens, T. E., & Jbabdi, S. (2016). Task-free MRI predicts individual differences in brain activity during task performance. *Science, 352*(6282), 216–220.
Tukey, J. W. (1977). *Exploratory data analysis*. Addison-Wesley Publishing Company.
Vakhtin, A. A., Ryman, S. G., Flores, R. A., & Jung, R. E. (2014). Functional brain networks contributing to the Parieto-Frontal Integration Theory of intelligence. *Neuroimage, 103*, 349–354.
Van Essen, D. C. (2005). A population-average, landmark- and surface-based (PALS) atlas of human cerebral cortex. *Neuroimage, 28*(3), 635–662.
Van Essen, D. C., Smith, S. M., Barch, D. M., Behrens, T. E., Yacoub, E., & Ugurbil, K. (2013). The WU-Minn Human Connectome Project: An overview. *Neuroimage, 80*, 62–79.
Van Essen, D. C., Ugurbil, K., Auerbach, E., Barch, D., Behrens, T. E., Bucholz, R., … Yacoub, E. (2012). The Human Connectome Project: A data acquisition perspective. *Neuroimage, 62*(4), 2222–2231.
Varley, R. (2007). Plasticity in high-order cognition: Evidence of dissociation in aphasia. *Behavioral and Brain Sciences, 30*(2), 171–172.
Volz, K. G., Schubotz, R. I., & von Cramon, D. Y. (2005). Variants of uncertainty in decision-making and their neural correlates. *Brain Research Bulletin, 67*(5), 403–412.